CO/CO_2 hydrogenation and ethylene hydroformylation over silica-supported PdZn catalysts

J. Araña [a], N. Homs [a,*], J. Sales [a], J.L.G. Fierro [b] and P. Ramirez de la Piscina [a,*]

[a] *Departament de Química Inorgànica, Universitat de Barcelona, Martí i Franqués 1-11, 08028 Barcelona, Spain*
E-mail: pilar.piscina@qi.ub.es
[b] *Instituto de Catálisis y Petroleoquímica, C.S.I.C., Cantoblanco, 28049 Madrid, Spain*

Received 10 August 2000; accepted 18 January 2001

Silica-supported PdZn catalysts have been studied in CO and CO_2 hydrogenation and in ethylene hydroformylation. The dilution of surface Pd by Zn lowers the hydrogenating capability of the catalysts and favours the production of higher hydrocarbons in CO hydrogenation. The catalyst with a molar ratio Pd : Zn = 3 showed an enhanced ability to insert CO into an M–alkyl bond; this catalyst produced higher oxygenates in the CO hydrogenation and was the most active in all reactions studied.

KEY WORDS: supported PdZn catalysts; supported PdZn alloy; vapour-phase hydroformylation; CO/CO_2 hydrogenation

1. Introduction

Catalysts based on Pd have been extensively studied both in the hydrogenation of organic substrates and in the syngas reaction. CO hydrogenation over Pd catalysts leads to methanol and methane. In these systems the influence of particle size, support and promoters on the activity and selectivity has been discussed from different points of view [1–6]. Alkaline metals have been studied as promoters and their effect has been interpreted in terms of changes in the adsorption of CO and a modification of the electronic structure of the metal. In general, the addition of small quantities of alkali metal increases the rate of methanol formation [4]. In some cases products other than methane and methanol have been obtained. For Pd–Li/CeO_2 catalysts, besides, higher hydrocarbons and ethanol were found [7,8]. In this area, less attention has been focussed on the effect of other metals that can form alloys with Pd, although there are reports of a change in the yield and selectivity when bimetallic sites are present [9]. In the hydrogenation of organic substrates supports like ZnO strongly modify the catalytic properties of palladium. Many proposals for the interaction of Pd particles with the reduced Zn from the support have been offered and the formation of bimetallic Pd–Zn particles has been claimed as responsible for the change in the catalytic performance [10,11]. Recently, we reported a DRIFT study on CO hydrogenation over a Pd–Zn silica-supported catalyst which showed unusual high selectivity to higher hydrocarbons and higher oxygenated products at 20 bar of total pressure and a $CO : H_2$ ratio of 1 [12]. Here we study the effect of Zn on the catalytic behaviour of silica-supported Pd catalysts. We have prepared and characterised Pd-based catalysts, including that mentioned above, with different Pd/Zn ratios, which were studied in CO and CO_2 hydrogenation at 30 bar, T range 543–598 K and different $H_2 : CO : CO_2$ ratios. Depending on the catalyst and the conditions, methane, methanol, higher alcohols and higher hydrocarbons were obtained. Taking into account that Pd is also active in the hydroformylation of olefins, this reaction was also tested in an attempt to relate the behaviour of catalysts to the presence of Zn and their structural characteristics.

* To whom correspondence should be addressed.

2. Experimental

2.1. Catalyst preparation

Three silica-supported catalysts were prepared with Pd : Zn molar compositions 1 : 0, 3 : 1 and 1 : 1.4; samples were labelled Pd/SiO_2, 3Pd1Zn/SiO_2 and 2Pd3Zn/SiO_2, respectively. Metallic precursors were $PdCl_2$ and $ZnCl_2$ and an aerosil-type silica (Degussa, BET surface area 200 $m^2\,g^{-1}$) was used as support. For catalysts preparation, first, silica was impregnated by the incipient-wetness method with acidified aqueous solutions of $PdCl_2$, and then the catalysts were dried under vacuum at 373 K. After that, Pd/SiO_2 was reduced at 573 K under flowing H_2. The preparation of 3Pd1Zn/SiO_2 is reported elsewhere [12]; a similar method was used for 2Pd3Zn/SiO_2 but changing the Pd/Zn ratio. After the Pd impregnation, Zn was impregnated by free adsorption from an acetone solution of $ZnCl_2$. Then, bimetallic catalysts were dried under vacuum at 373 K and reduced at 673 K under flowing H_2. Chemical analyses of the catalysts appear in table 1.

2.2. Catalyst characterisation

X-ray diffraction patterns were obtained by collecting at a step width of 0.02° in the 2θ range of interest us-

1011-372X/01/0400-0183$19.50/0

Table 1
Chemical composition (wt%), binding energies (eV) of core electrons and XPS atomic ratios for silica-supported palladium catalysts.[a]

Catalyst	Pd (%)	Zn (%)	Pd $3d_{5/2}$	Zn $2p_{3/2}$	Pd/Si (XPS)	Zn/Si (XPS)
Pd/SiO_2	2.80	–	335.2	–	0.0047	–
$3Pd1Zn/SiO_2$	2.53	0.52	336.0	1022.2[b]	0.052	0
$2Pd3Zn/SiO_2$	2.07	1.76	335.9	1022.4	0.004	0.0118

[a] The Si 2p peak at a binding energy of 103.4 eV was taken as an internal standard.
[b] Obtained after sputering with Ar^+.

ing a Siemens D-500 X-ray diffractometer equipped with a graphite monochromator and Cu target. Particle size was estimated by using the Scherrer formula at various high-intensity reflections corrected from Cu $K_{\alpha 2}$ radiation.

CO and H_2 chemisorption were carried out in a static volumetric apparatus at 298 K. Reduced catalysts were pelleted and introduced in the chemisorption cell. They were then re-reduced under flowing H_2 at 673 K for 2 h and outgassed at the same temperature for 3 h. Two isotherms were determined for each adsorbate, using equilibrium pressures of up to 40 Torr (1 Torr = 133.33 Pa). Once the first isotherm was obtained, which gave the total uptake of gas at 298 K, samples were evacuated for 1 h at room temperature, and then the second isotherm was obtained to determine the amount of physisorbed gas.

Infrared spectra were acquired with a Nicolet 520 Fourier transform instrument at 2 cm^{-1} resolution by collecting 100 scans. Special greaseless vacuum cells with CaF_2 windows which allowed thermal treatments were used. Samples were pelleted and introduced into the infrared cells. Before the chemisorption experiments, they were re-reduced under H_2 at 673 K for 1 h.

XP (X-ray photoelectron) spectra were acquired with a VG ESCALAB 200R electron spectrometer equipped with a hemispherical electron analyser and a Mg K_α X-ray source ($h\nu = 1253.6$ eV, 1 eV = 1.602×10^{-19} J). The samples were mounted on a sample rod placed in a pre-treatment chamber and pre-reduced in H_2 *in situ* at 673 K for 2 h. The C 1s, Si 2p, Cl 2p, Pd 3d and Zn $2p_{3/2}$ peaks, and in some cases the Zn_{LMM} Auger transition, were recorded. The intensities of the peaks were estimated by calculating the integral of each peak after smoothing and subtraction of an S-shaped background, and fitting the experimental curve to a combination of Gaussian and Lorentzian lines (G/L = 9–27%). The binding energy of the Si 2p peak at 103.4 eV was taken as an internal standard. In some cases, samples were Ar^+-sputtered using a beam of Ar^+ ions accelerated at 1.7 keV.

2.3. Catalytic activity

The catalytic activity measurements were carried out using a stainless-steel flow microreactor 8 cm long (i.d. 6.4 mm). The reaction pressure was maintained by means of a back-pressure regulator, at 30 bar. The flow of reactants (CO, H_2, CO_2 or C_2H_4) was adjusted by individual mass flow controllers. Usually, 0.25–0.5 g of catalyst was used in the measurement of catalytic activity. Reduced catalysts were re-reduced in the reactor at 673 K under flowing H_2 at atmospheric pressure by increasing temperature at 4 K min^{-1} and maintaining 673 K for 1 h. The reactor was allowed to cool under flowing hydrogen until the reaction temperature was reached. The reactant flows and total pressure were then adjusted to desired values. For each catalyst first hydrogenation of CO and CO_2 were carried out and subsequently the hydroformylation of ethylene was studied. After about 16 h on stream, the first data point was taken. Following a change in reaction conditions a minimum of 4 h was allowed for the catalyst to reach steady state. The reactor effluent was analysed by gas chromatography using a 3400 Varian gas chromatograph equipped with an automated on-line gas sample valve and flame ionisation and thermal conductivity detectors. Reactants and products were separated in a Carbograph column (2 m) and a molecular sieve column (1 m). Response factors and retention times were calibrated using standards.

3. Results and discussion

3.1. Characterisation of catalysts

Catalysts were characterised by XRD, XP spectroscopy and H_2 and CO chemisorption. The XRD patterns of catalysts after reaction are shown in figure 1; for comparative purposes only the region $2\theta = 35°$–$50°$ is shown. The pattern of Pd/SiO_2 corresponds well to the presence of palladium particles of about 18 nm. The pattern of $2Pd3Zn/SiO_2$ indicates the presence of PdZn phase (particle size 13 nm). From a comparison between the XRD pattern of $3Pd1Zn/SiO_2$ and those of $2Pd3Zn/SiO_2$ and Pd/SiO_2 the presence of both Pd and PdZn phases can be inferred in the $3Pd1Zn/SiO_2$ sample.

The Si 2p, Pd 3d, Zn 2p and Cl 2p core-level spectra were recorded for all samples. Small traces of chlorine species were detected only for Pd/SiO_2. In the Pd 3d region a single component was obtained for all catalysts (see figure 2). The binding energies of the most intense Pd $3d_{5/2}$ peak are given in table 1. The value obtained for the Pd/SiO_2 catalyst (335.2 eV) corresponds to that reported for metallic Pd or silica-supported Pd [13,14]. The other two catalysts showed higher Pd $3d_{5/2}$ binding energies: a shift of ca. 0.8 eV. A large positive shift in the Pd $3d_{5/2}$ XPS transition had been taken as a clear evidence of formation of Pd–Zn alloys in Pd/ZnO catalysts [15,16]. The formation of Pd–Zn bonds increases the binding energy of the core and valence levels of Pd and reduces the binding energy of the core and valence levels of Zn. However, the Zn core levels are somewhat less sensitive to alloy formation than the Pd core levels [17].

Zn $2p_{3/2}$ level spectra obtained for $2Pd3Zn/SiO_2$ catalyst showed a single signal centred at 1022.2 eV, which did not allow us to discern the Zn oxidation state. In contrast, $3Pd1Zn/SiO_2$ did not show any peak assigned to Zn 2p level,

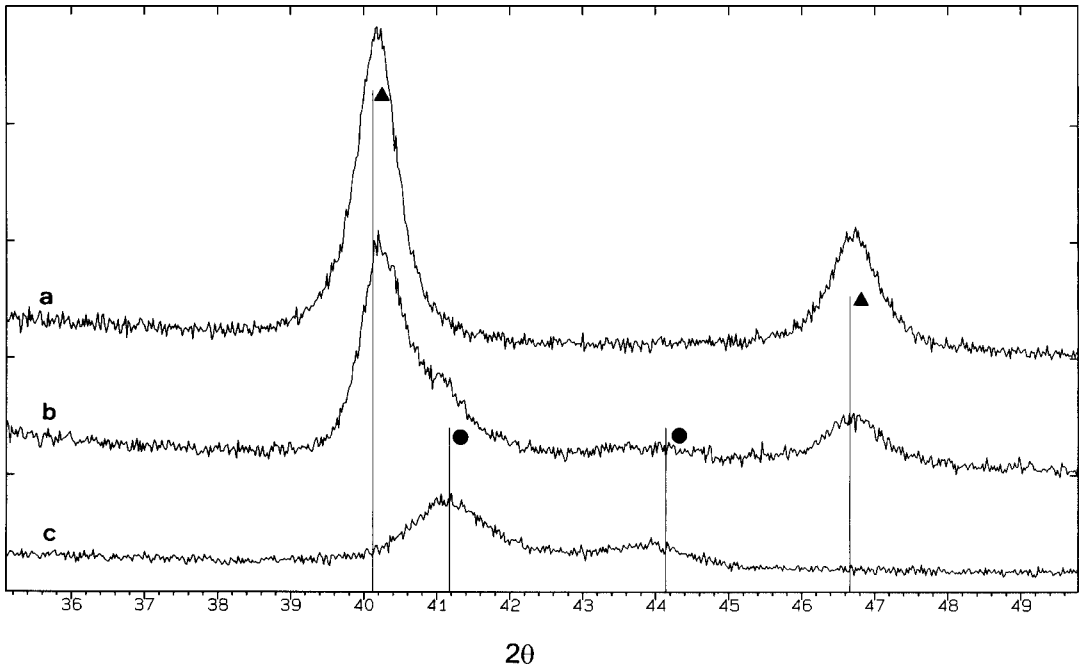

Figure 1. XRD patterns of the catalysts: (a) Pd/SiO_2, (b) 3Pd1Zn/SiO_2 and (c) 2Pd3Zn/SiO_2; (▲) Pd phase and (●) PdZn phase.

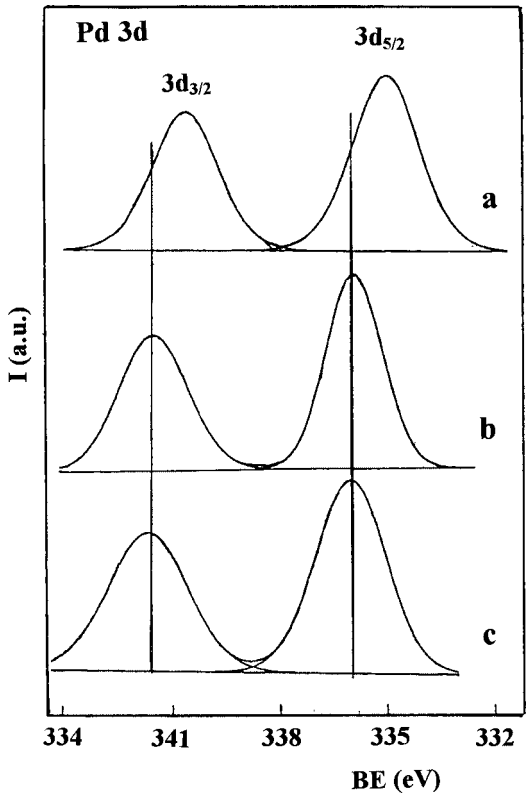

Figure 2. XP core-level spectra of the catalysts: (a) Pd/SiO_2, (b) 3Pd1Zn/SiO_2 and (c) 2Pd3Zn/SiO_2.

and it was only possible to discern the Zn 2p peak after sputtering with Ar^+. Then, this sample showed a signal centred at 1022.4 eV but broader than that of 2Pd3Zn/SiO_2, probably due to the surface heterogeneity produced by the Ar^+ sputtering. As it was not possible to discern the Zn oxidation state by XPS, Auger spectra corresponding to Zn_{LMN} were recorded. A broad asymmetric peak was observed that was deconvoluted in two signals assigned to Zn^{2+} and Zn^0. However, an analysis of a sample of ZnO taken as a blank showed a similar Auger spectrum.

Figure 3 shows the adsorption isotherms of H_2 (figure 3(a)) and CO (figure 3(b)) for bimetallic catalysts. 2Pd3Zn showed a very low capability to chemisorb H_2 but a non-negligible CO chemisorption, whereas 3Pd1Zn/SiO_2 chemisorbed in a significant extent both H_2 and CO. Taking into account that for 2Pd3Zn/SiO_2 the Pd/Zn surface atomic ratio determined by XPS was 0.34, chemisorption data may be interpreted as a dilution effect of surface Pd by Zn. The decrease in the number of adjacent Pd atoms produced a decrease in the amount of dissociatively chemisorbed H_2. When 2Pd3Zn/SiO_2 was exposed to CO, a band at 2040 cm^{-1} corresponding to terminal CO was obtained, which was more intense than another assigned to bridging CO (ν(CO) = 1902 cm^{-1}), which is consistent with the dilution effect. This catalyst also exhibited a band around 1680 cm^{-1} suggesting a C- and O-bonded carbon monoxide species. When CO adsorption was carried out over 3Pd1Zn/SiO_2 a single band at 1905 cm^{-1} was obtained, in good agreement with the presence of adjacent Pd atoms, favouring a bridged-CO coordination. In this case a band in the low frequency region was also observed. This band, at 1696 cm^{-1}, may also have arisen from a CO bonded to two surface sites through C and O atoms. XRD had indicated the presence of the PdZn bimetallic phase in both 2Pd3Zn and 3Pd1Zn. However, XPS analysis indicated the absence of Zn but the presence of alloyed Pd on the surface of the 3Pd1Zn/SiO_2 catalyst. Taking into account all these data, we propose for 3Pd1Zn/SiO_2 a decoration of PdZn bimetallic particles, at least partially by Pd atoms.

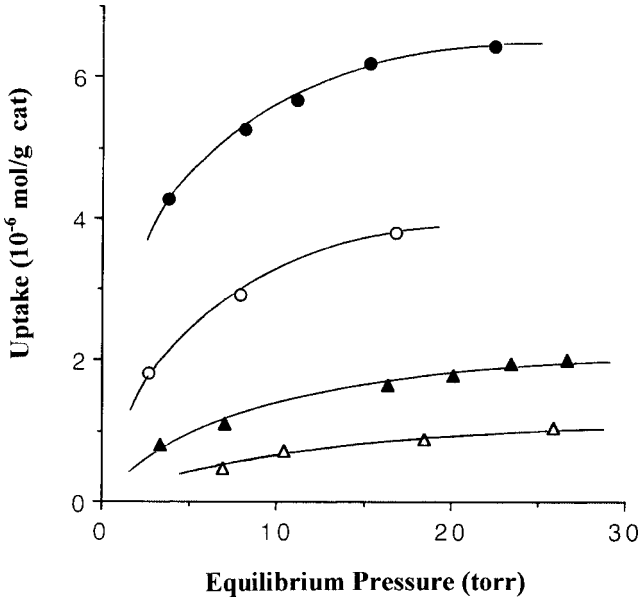

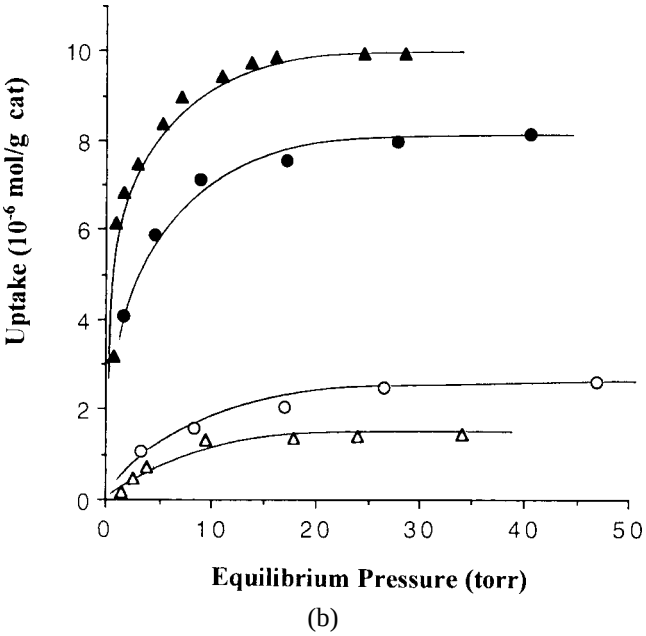

Figure 3. (a) Room temperature hydrogen chemisorption. (b) Room temperature CO chemisorption. Catalysts: (▲, △) 2Pd3Zn/SiO_2 and (●, ○) 3Pd1Zn/SiO_2 (filled symbols total adsorption, empty symbols weak adsorption).

3.2. Catalytic behaviour

To study the effect of Zn on the catalytic properties of Pd, three reactions were studied: CO hydrogenation, CO_2 hydrogenation and ethylene hydroformylation. The CO hydrogenation was carried out over the catalysts at 30 bar, temperatures between 548 and 598 K and H_2 : CO ratios ranging from 3 to 0.5. In general, for high H_2 : CO ratios (H_2 : CO = 2 and 3) an increase of temperature produced an increase in the activity, although the behaviour of each catalyst was different. 3Pd1Zn was the most active in any experimental condition used, while Pd/SiO_2 showed a very low activity. The data are summarised in table 2.

Table 2
Specific activity of catalysts in the CO hydrogenation (H_2 : CO = 2 : 1) at 30 bar.

Catalyst	T (K)	P (bar)	mol_{CO} converted $mol_{Pd}^{-1}\,h^{-1}$
Pd	573	30	0.8
2Pd3Zn	573	30	12.5
	598	30	31.4
3Pd1Zn	573	30	39.3
	598	30	101.4

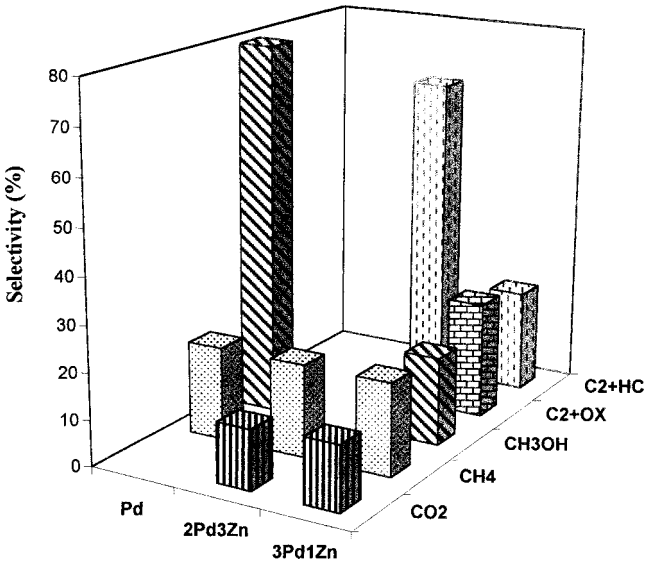

Figure 4. Selectivity of catalysts in the CO hydrogenation at 30 bar, H_2 : CO = 2 : 1, T = 573 K.

Pd/SiO_2 produced methanol and methane, 2Pd3Zn/SiO_2 produced (besides CO_2), only hydrocarbons (C_1–C_6) and the most active catalyst, 3Pd1Zn/SiO_2, produced CO_2, methane, methanol, higher hydrocarbons (C_2–C_6), higher alcohols (ethanol, propanol) and acetaldehyde; the selectivity depended on the conditions. In the figure 4 is illustrated the selectivity of catalysts to the different products at 573 K and H_2 : CO = 2.

As stated above, over 2Pd3Zn C_1–C_6 hydrocarbons were produced. An analysis of products obtained at 573 or 598 K was consistent with the Anderson–Schulz–Flory kinetics throughout the range of hydrocarbons produced (C_1–C_6). The plot of log W_p/p *versus* p gave straight lines which allowed calculation of the propagation factor α, which ranged from 0.5–0.7 at 573 K to 0.4–0.6 at 593 K (figure 5). Apparent activation energy (E_a) for methane was calculated from Arrhenius plots between 548 and 598 K and different H_2 : CO ratios. The values obtained, 24.5 ± 2 kcal mol^{-1}, were similar to those reported for Pd/SiO_2 catalysts with Pd content 1.5–2% (w/w) [18,19].

3Pd1Zn/SiO_2 gave a wider diversity of products, the selectivity changing to hydrocarbons or oxygenates as a function of reaction conditions (figure 6). Higher selectivity to

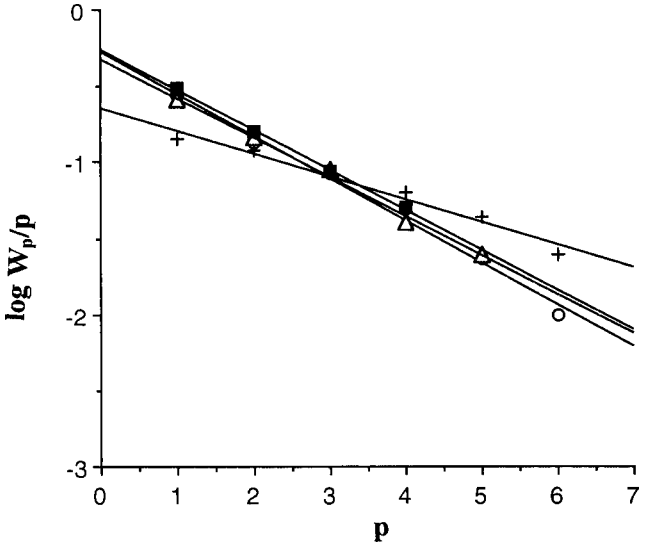

(a)

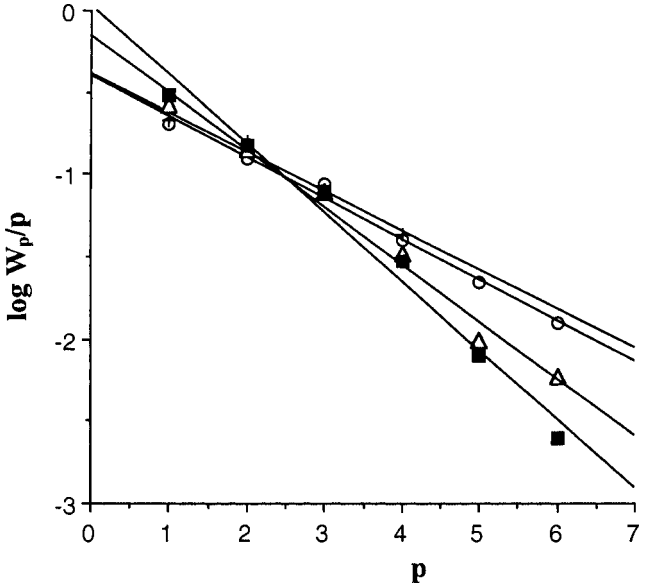

(b)

Figure 5. ASF plot of hydrocarbons obtained with the 2Pd3Zn catalyst at $P = 30$ bar and different $H_2:CO$ ratios: (○) 0.5 : 1, (+) 1 : 1, (△) 2 : 1 and (■) 3 : 1. Reaction temperature (a) 573 and (b) 598 K.

methanol and higher oxygenates (C_{2+ox}) was produced at high H_2/CO ratios ($H_2:CO = 2$ and 3), whereas selectivity to higher hydrocarbons was greater at lower $H_2:CO$ ratios ($H_2:CO = 0.5$ and 1). In general a decrease in the temperature increased selectivity to oxygenates.

Product distribution was analysed from the Anderson–Schulz–Flory plots, separately for hydrocarbons and oxygenated products. Hydrocarbons followed ASF kinetics in the whole range obtained, C_1–C_5, whereas oxygenates (studied in the range C_1–C_3) did not. The α values obtained for the hydrocarbon distribution were in the range 0.3–0.4 at 573 K and 0.2–0.4 at 593 K.

The apparent E_a values for 3Pd1Zn/SiO$_2$ between 548 and 598 K were: 17.5 ± 2 kcal/mol for CH_3OH, 16.0 ±

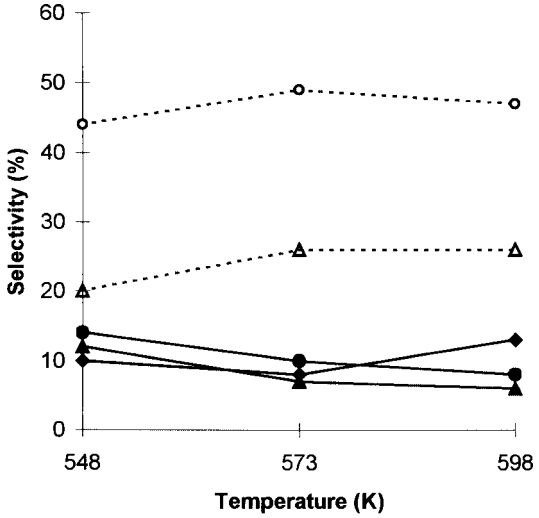

(a)

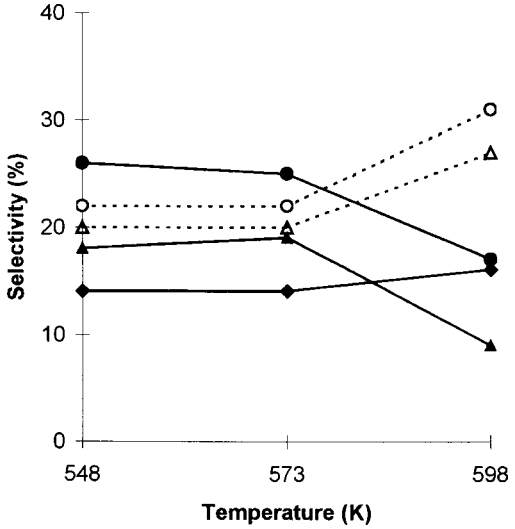

(b)

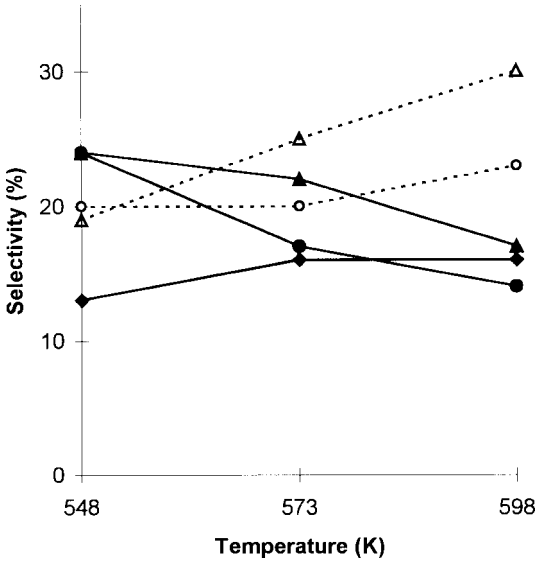

(c)

Figure 6. Selectivity of 3Pd1Zn catalyst in the CO hydrogenation as a function of T at $P = 30$ bar. $H_2:CO$ ratios: (a) 1 : 1, (b) 2 : 1 and (c) 3 : 1. Products: (●) C_{2+ox}, (○) C_{2+HC}, (▲) CH_3OH, (△) CH_4 and (♦) CO_2.

2 kcal/mol for C_{2+ox} and 25.2 ± 2 kcal/mol for CH_4. E_a for methane is close to that of 2Pd3Zn, and the E_a for methanol corresponds to values reported for Pd/SiO_2 [18,19].

From the characterisation data of 2Pd3Zn and its catalytic behaviour it is possible to relate the C_{2+HC} production to the presence of alloyed Pd. In fact, silica-supported palladium–tin catalysts with only bimetallic Pd_xSn_y phases show similar behaviour [20].

Catalysts were tested in CO_2 hydrogenation at 30 bar and temperatures of 573 and 598 K. In table 3 are summarised the data for the $3Pd1Zn/SiO_2$ catalyst, which was the only one active under the reaction conditions used. The results obtained for the hydrogenation of $CO_2 + CO$ mixtures were similar to that of CO hydrogenation. However, when only CO_2 was hydrogenated the activity was much lower. The high selectivity to CO indicated that reverse water–gas shift reaction took place. In the same experimental conditions CO was not produced over either Pd/SiO_2 or $2Pd3Zn/SiO_2$. The effect of support for Pd catalysts on CO_2 hydrogenation had been studied [21] and no activity in the RWGS reaction had been found for silica-supported Pd catalysts. This was taken as proof that metallic palladium alone does not catalyse the RWGS reaction and it was considered that this reaction proceeded on the surface of oxides like Al_2O_3, TiO_2 or ZnO, where CO_2 is adsorbed and reacts with spillover hydrogen atoms from metal particles to form formate species, intermediates in the RWGS reaction. In our case, all three catalysts are silica-supported, so another explanation is required.

Table 3
Hydrogenation of $CO + CO_2$ mixtures over 3Pd1Zn catalyst at 30 bar.

$H_2:CO_2:CO$	T (K)	Specific activity[a]	Selectivity[b] (%)				
			CO	CH_4	C_{2+HC}	MeOH	C_{2+ox}
2:1:1	573	45.9	–	32	43	13	12
2:1:1	598	82.1	–	34	38	14	14
1:1:0	573	1.4	79	16	4	1	0
1:1:0	598	3.3	76	17	4	3	0
3:1:0	573	1.1	65	20	14	1	0
3:1:0	598	2.2	63	21	14	2	0

[a] Mole of $CO + CO_2$ reacted per mole Pd per hour.
[b] Based on mole of $CO + CO_2$ converted.

A study by FTIR spectroscopy of CO_2 interaction with the catalysts revealed large differences in the behaviour of catalysts. When CO_2 came into contact with the catalysts a band centred at 2343 cm^{-1} appeared, which was eliminated after vacuum treatment at room temperature and was assigned to physisorbed CO_2 on SiO_2. Only the $3Pd1Zn/SiO_2$ catalyst showed a band at 2339 cm^{-1}, which remained after vacuum treatment at room temperature. When this catalyst came into contact with a $CO_2 + H_2$ mixture at room temperature bands at 2028 and 1900 cm^{-1} due to coordinated CO (terminal and bridging respectively) appeared, whereas the band at 1696 cm^{-1} was not present.

As stated above, when the CO hydrogenation was carried out over the $3Pd1Zn/SiO_2$ catalyst, higher alcohols were produced. In this reaction a key step is the CO insertion in an M–alkyl bond, and this may be a common step of the hydroformylation reaction. In order to attempt a comparison between both reactions over these palladium systems, the hydroformylation reaction of ethylene was tested. Table 4 compiles the results obtained over the catalysts between 433 and 473 K at 30 bar and $C_2H_4:CO:H_2 = 1:1:1$. The most active catalyst was $3Pd1Zn/SiO_2$, which was also the most active in the hydrogenation of CO and CO_2, and the only one which produced higher oxygenates in the CO hydrogenation. When ethane produced is excluded in the calculation of selectivity, Pd and $3Pd1Zn/SiO_2$ showed similar values of selectivity to oxygenates, however the hydrogenating capacity of Pd/SiO_2 was higher than that of $3Pd1Zn/SiO_2$, and most of ethylene was hydrogenated to ethane over the monometallic catalyst. Both catalysts showed by XPS only Pd as metallic phase on the surface, the Pd/Si ratio being tenfold higher for $3Pd1Zn/SiO_2$ than for Pd. However, they differ in the BE of Pd. On the other hand, $2Pd3Zn/SiO_2$ showed low hydrogenation of ethylene, consistent with the low capability of hydrogen chemisorption shown by this catalyst indicating the dilution effect of Zn on Pd. This catalyst showed the highest selectivity to higher hydrocarbons in both CO hydrogenation and hydroformylation of ethylene.

Table 4
Hydroformylation of ethylene over the catalysts at 30 bar of total pressure and $C_2H_4:CO:H_2 = 1:1:1$.

Catalyst	T (K)	Specific activity[a]	Selectivity[b] (%)		Oxygenate selectivity (%)			C_2H_6[c] (%)
			C_{ox}	HC	$C_{3\text{-al}}$	$C_{3\text{-ol}}$	$C_{4\text{-al}}$	
Pd	433	5.2	92	8	60	40	0	80.7
Pd	453	6.0	90	10	57	43	0	87.6
Pd	473	36.8	92	8	49	47	4	91.3
2Pd3Zn	433	1.5	59	41	100	0	0	5.4
2Pd3Zn	453	3.8	73	27	79	19	2	7.6
2Pd3Zn	473	5.4	77	23	78	22	0	8.8
3Pd1Zn	433	26.5	91	9	77	17	6	49.1
3Pd1Zn	453	28.6	94	6	48	43	9	51.2
3Pd1Zn	473	40.1	88	12	42	48	10	59.3

[a] Mole CO reacted to oxygenates per mole Pd per hour.
[b] Selectivity to oxygenates and hydrocarbons, except ethylene and ethane.
[c] C_2H_4 hydrogenated to C_2H_6.

4. Summary and conclusions

Our results show that the selectivity in the CO hydrogenation reaction over silica-supported palladium-based catalysts can be regulated. 2Pd3Zn/SiO_2 is a Fischer–Tropsch catalyst. Over this catalyst, the CH_x surface species produced after CO dissociation evolve to higher hydrocarbons, in contrast to Pd, which is a methanol catalyst and only produces CH_4 as hydrocarbon. The structural characteristics of 2Pd3Zn/SiO_2, in which surface palladium is diluted by Zn, determine the low capability of this catalyst to hydrogenate, which determine its catalytic behaviour. 3Pd1Zn/SiO_2 showed the highest ability to insert CO as it was evidenced in the hydroformylation reaction; this catalyst was the only one which produced higher alcohols in the CO hydrogenation reaction.

Acknowledgement

We thank CICYT (MAT96-0859-C02 and MAT1999-0477) and CIRIT (1997SGR-00265 and 1999SGR-00044) for financial support, Johnson–Matthey is gratefully acknowledged for a loan of palladium salt.

References

[1] J.P. Hindermann, G.J. Hutchings and A. Kiennemann, Catal. Rev. Sci. Eng. 35 (1993) 1.
[2] S. Ichikawa, H. Poppa and M. Boudart, J. Catal. 91 (1985) 1.
[3] A. Gotti and R. Prins, Catal. Lett. 37 (1996) 143.
[4] A.M. Kazi, B. Chen, J.G. Goodwin, J.G. Marcelin, N. Rodriguez and R.T.K. Barker, J. Catal. 157 (1995) 1.
[5] V. Ponec, in: *Metal–Suport and Metal Additive Effects in Catalysis*, eds. B. Imelik et al. (Elsevier, Amsterdam, 1982) p. 63.
[6] Z. Karpinski, Adv. Catal. 37 (1990) 45.
[7] C. Diagne, H. Idriss, I. Pepin, J.P. Hindermann and A. Kiennemann, Appl. Catal. 50 (1989) 43.
[8] C. Diagne, H. Idriss, J.P. Hindermann and A. Kiennemann, Appl. Catal. 51 (1989) 165.
[9] T. Fukushima, K. Araki and M. Ichikawa, J. Chem. Soc. Chem. Commun. (1986) 148.
[10] P.S. Wehner and B.L. Gustafson, J. Catal. 135 (1992) 420.
[11] B.E. Green, C.S. Sass, L.T. Germinario, P.S. Wehner and B.L. Gustafson, J. Catal. 140 (1993) 406.
[12] J. Araña, N. Homs, J. Sales and P. Ramírez de la Piscina, J. Mol. Catal. A, in press.
[13] G.E. Muilenberg, ed., *Handbook of X-ray Photoelectron Spectroscopy*, Physical Electronics (Perkin–Elmer, Eden Prairie, MN, 1990).
[14] T.H. Fleisch, R.F. Hicks and A.T. Bell, J. Catal. 87 (1984) 398.
[15] N. Iwasa, S. Masuda, N. Ogawa and N. Takezawa, Appl. Catal. A 125 (1995) 145.
[16] Z. Zsoldos, A. Sárkány and Z. Guczi, J. Catal. 145 (1994) 235.
[17] J.A. Rodriguez, J. Phys. Chem. 98 (1994) 5758.
[18] Y.A. Ryndin, R.F. Hicks, A.T. Bell and Y.I. Yermakov, J. Catal. 70 (1981) 287.
[19] R.F. Hicks and A.T. Bell, J. Catal. 91 (1985) 104.
[20] J. Araña, P. Ramírez de la Piscina, J. Sales and N. Homs, unpublished results.
[21] T. Fujitani, M. Saito, Y. Kanai, T. Watanabe, J. Nakamura and T. Uchijima, Appl. Catal. A 125 (1995) L199.